Fluorine-18-Antimyosin Monoclonal Antibody Fragments: Preliminary Investigations in a Canine Myocardial Infarct Model

Michael R. Zalutsky, Pradeep K. Garg, Scott H. Johnson, Hidetoshi Utsunomiya, and R. Edward Coleman

Department of Radiology, Section of Nuclear Medicine and Department of Surgery, Duke University Medical Center, Durham, North Carolina

The purpose of this study was to determine in a canine model whether selective myocardial infarct uptake of ^{18}F-labeled antimyosin monoclonal antibody fragments could be achieved in a time frame compatible with the short half-life of this nuclide. Antimyosin monoclonal antibody fragments were labeled with ^{18}F using a succinimidyl [^{18}F]fluorobenzylamine ester acylation agent. Six dogs had myocardial infarction induced by coronary artery occlusion and were reperfused prior to the intravenous administration of 0.6–4.7 mCi of ^{18}F-labeled F(ab')$_2$ (two dogs) or Fab (four dogs). Analysis of tissues obtained 2–4 hr after antibody administration revealed infarct:normal myocardium uptake ratios as high as 14–21:1 for F(ab')$_2$ and 9–12:1 for Fab. Even with Fab, however, prolonged ^{18}F activity in the blood pool interfered with delineation of infarcts by PET imaging. In one dog, perfusion imaging with [^{13}N]ammonia before antimyosin administration was performed, and regions of normal and ischemic myocardium were determined. With these regions of interest, infarct:normal myocardium uptake ratios calculated from the ^{18}F-labeled Fab images increased from 1.5:1 at 1 hr to 4.0:1 at 5 hr. We conclude that ^{18}F-labeled antimyosin fragments may be of value for hot-spot imaging of damaged myocardium with PET; however, blood-pool subtraction techniques will probably be required.

J Nucl Med 1992; 33:575–580

Among the most active areas of positron emission tomography (PET) is the application of this technology to the evaluation of heart disease. Indeed, at some PET centers, including those with cyclotrons, cardiac indications account for the majority of patient studies (*1*). A number of tracers are available for the assessment of regional myocardial perfusion including ^{13}N-ammonia, ^{15}O-water and ^{82}Rb (*2–4*). Radiopharmaceuticals for the evaluation of myocardial metabolic status include ^{11}C-palmitate, [^{18}F]fluoro-2-deoxyglucose and ^{11}C-acetate (*5–7*). In addition, [^{18}F]misonidazole is being evaluated for use in the delineation of hypoxic myocardial tissue (*8,9*). Although the diagnostic armamentarium available for cardiac PET is extensive, a relatively unexplored area is the utilization of a PET tracer for infarct-avid imaging.

One of the most promising approaches for "hot-spot" imaging of acute myocardial infarction is the use of radiolabeled antimyosin monoclonal antibody (Mab) fragments. Antimyosin F(ab')$_2$ and Fab fragments have been labeled with ^{131}I (*10*), ^{99m}Tc (*11*), and ^{111}In (*12*) and have demonstrated localization in experimental models of myocardial infarction. Most clinical studies have utilized ^{111}In-labeled Fab immunoscintigraphy and shown specific delineation of necrotic myocardium (*13,14*). Antimyosin Mab fragments, in addition to their use in the evaluation of myocardial infarction, may also be of value in detecting rejection after heart transplantation (*15*) and in imaging of acute myocarditis (*16*).

Antimyosin Mab fragments labeled with a positron-emitting nuclide might permit the simultaneous exploitation of antimyosin uptake specificity in damaged myocardium and of imaging advantages and quantitative capabilities inherent in PET. Because Mab fragments are cleared from the blood-pool more slowly than most tracers used in PET, a longer lived nuclide would be advantageous, permitting imaging at later time points when contrast between myocardium and blood should be increased.

Of the positron-emitting nuclides that are available routinely, ^{18}F has the longest half-life (1.83 hr) and thus may be of value as a label for Mab fragments. Recently, we described a method for labeling antimyosin fragments with ^{18}F that utilized *N*-succinimidyl 8-[(4'-[^{18}F]fluorobenzyl)amino]suberate ([^{18}F]SFBS) as the labeled acylation agent (*17*). Antimyosin F(ab')$_2$ and Fab fragments could be labeled with ^{18}F with good retention of immunoreactivity. The present study was undertaken in a canine model to determine whether preferential myocardial infarct uptake of ^{18}F-labeled antimyosin fragments could be achieved in a time frame compatible with the half-life of ^{18}F.

MATERIALS AND METHODS

Fluorine-18 Labeling of Antimyosin Mab Fragments

Production of the mouse Mab (R11D10) directed against cardiac myosin used in these studies has been described by Khaw

Received Aug. 6, 1991; revision accepted Dec. 4, 1991.

For reprints contact: Michael R. Zalutsky, PhD, Duke University Medical Center, Department of Radiology, Box 3808, Durham, NC 27710.

et al. (*11*). The F(ab')$_2$ and Fab fragments of this Mab were provided by Dr. David Shealy of Centocor (Malvern, PA).

A detailed description of the methods used for labeling these Mab fragments with ^{18}F has been reported previously (*17*). Briefly, aqueous [^{18}F]fluoride was produced by proton bombardment of ^{18}O-water using a small-volume silver target. The protein acylation agent [^{18}F]SFBS was prepared in three steps. After conversion of aqueous [^{18}F]fluoride ion to tetrabutylammonium [^{18}F]fluoride, 4-[^{18}F]fluorobenzonitrile was prepared by fluoro for nitro exchange in 4-nitrobenzonitrile. Conversion to 4-[^{18}F]fluorobenzylamine was accomplished by treatment of the labeled product with lithium aluminum hydride. Reaction of 4-[^{18}F] fluorobenzylamine with disuccinimidyl suberate for 5 min at room temperature yielded [^{18}F]SFBS. The [^{18}F]SFBS was used either in unpurified form or was purified by high-pressure liquid chromatography (HPLC) using a silica gel column eluted with ethyl acetate.

After evaporation of the organic solvent containing the [^{18}F] SFBS in a glass vial, 1.0–1.1 mg of antimyosin Mab fragment (Fab, 2.7 mg/ml; F(ab')$_2$, 5.6 mg/ml) in borate buffer (pH 8.5) was added and reacted for 15 min at room temperature. After terminating the reaction by the addition of 0.2 M glycine, the ^{18}F-labeled antimyosin Mab fragment was purified by chromatography over a 1 × 10 cm Sephadex G-25 column eluted with phosphate-buffered saline. Protein-associated ^{18}F activity, determined by precipitation with 20% trichloroacetic acid, was between 96%–99% for all preparations.

A myosin Sepharose column was used to determine the immunoreactivity of the ^{18}F-labeled antimyosin F(ab')$_2$ and Fab fragments. After adding about 10 ng of labeled fragment to a 1-ml column, the column was washed with 0.5% human serum albumin in phosphate-buffered saline and then stripped with glycine (pH 2.5). After counting the ^{18}F activity present in aliquots of the saline and glycine solutions, immunoreactivity was calculated as the activity eluted in glycine divided by the activity eluted in saline plus glycine.

Animal Preparation

Six adult mongrel dogs weighing between 20–30 kg were studied. Animals were anesthetized with sodium pentobarbital (30 mg/kg), intubated, and mechanically ventilated. Catheters were positioned in the right femoral artery for pressure monitoring and in the right femoral vein for blood sampling. The electrocardiogram was monitored continuously. A left thoracotomy was performed through the sixth interspace and a pericardial cradle was fashioned. A reversible ligature was positioned around the proximal left circumflex or left anterior descending coronary artery.

Experimental Protocol

A lidocaine bolus (25 mg) was administered and an intravenous infusion of lidocaine (0.5 mg/min) was started. The coronary ligature was tightened to produce total occlusion for a period of 2–3 hr, after which the ligature was released for reperfusion. After 30 min of reperfusion, the animals were injected intravenously with 0.6–2.8 mCi of ^{18}F-labeled antimyosin F(ab')$_2$ (two dogs) or 4.3–6.0 mCi of ^{18}F-labeled antimyosin Fab fragment (four dogs).

Serial PET images of the ^{18}F-labeled Mab fragments were obtained of Dogs 2–6 (Table 1) with five scans of 1 min each, one scan of 10 min, three scans of 15 min each, followed by 30-min scans thereafter. The total duration of image acquisition was 120 min for Dogs 2–4, 210 min for Dog 5, and 315 min for Dog 6. For Dogs 1–5, a 1.0 ml venous blood sample was withdrawn into a heparinized vial immediately prior to killing them.

TABLE 1
Evaluation of ^{18}F-Labeled Antimyosin Mab Fragments in Canine Infarct Model

Number*	Fragment	HPLC of SFBS	Dose (mCi)	Specific activity (mCi/mg)	Immunoreactivity (%)
1	F(ab')$_2$	No	2.8	3.7	33
2	F(ab')$_2$	No	0.6	2.3	79
3	Fab	Yes	4.3	6.8	54
4	Fab	No	6.0	7.7	28
5	Fab	Yes	4.7	6.9	84
6	Fab	Yes	4.7	5.5	84

* PET imaging performed on Dogs 2–6; tissue and blood sampling performed on Dogs 1–5.

When PET imaging was completed, thioflavin-S was administered; 30 sec later, the animal was killed with a large dose of pentobarbital. The heart was excised rapidly and sliced into five short-axis sections. The sections were stained with triphenyltetrazolium chloride to identify three regions of interest (ROIs): area of infarction, border zone, and area of normal myocardium. Two short-axis sections were divided into the three ROIs and 0.5–1.0-g samples were obtained from the endocardium, midmyocardium, and epicardium from each region.

Blood and tissue samples were weighed and then counted for ^{18}F activity using an LKB 1282 automated gamma counter. A correction was applied for isotopic decay of the ^{18}F. The percent injected dose per gram (%ID/g) blood or tissue was calculated by comparison with ^{18}F injection standards of appropriate count rate. Infarct-to-normal myocardium tissue uptake ratios were also calculated from these counting data.

PET Data Acquisition and Processing

Blank scans were obtained and the animals were placed in the gantry of an ECAT III PET tomograph (CTI, Knoxville, TN) with the collimators set to give a slice thickness of 16 mm at full width half maximum. The animals were positioned with the use of lasers to assure that the myocardium distal to the circumflex artery was in the field of view of the detectors. Three transmission planes (two direct planes, one cross plane) were obtained for 10 min using ^{68}Ga-EDTA. In one animal (Dog 6), ^{13}N-ammonia (15 mCi) was administered during occlusion and after reperfusion to evaluate perfusion. The perfusion images were obtained starting 3 min after tracer administration and were acquired for 5 min. The first ^{13}N-ammonia image was obtained 5 min after occlusion, and the second image was obtained 120 min later. In this animal, ^{18}F-labeled antimyosin Fab (4.7 mCi) was administered 20 min after reperfusion, and images were obtained as described above.

The ^{13}N-ammonia and ^{18}F-labeled antimyosin Mab fragment images were evaluated using 12 ROIs assigned manually to the cross-sectional images. In the animal receiving both radiotracers, the same ROIs were used on both sets of images. Ratios of activity

in the selected regions of an image were calculated on a cpm/pixel basis.

RESULTS

In general, about 8 mCi of ^{18}F-labeled antimyosin Mab fragment was obtained per 100 mCi of [^{18}F]fluoride in a total synthesis time of 80–90 min. With the exception of Dog 2, this permitted the administration of 2.8–6.0 mCi of ^{18}F-labeled Mab fragment. Immunoreactivity, determined using a myosin affinity column, was higher for preparations using HPLC-purified [^{18}F]SFBS (no HPLC, 47%±28%; HPLC, 74%±17%).

Tissue distribution studies were performed on Dogs 1–5 to determine whether preferential uptake of ^{18}F-labeled Mab fragments in damaged myocardium could be achieved in a time frame compatible with the short half-life of ^{18}F. Normal, border zone, and infarcted regions were determined using triphenyltetrazolium chloride. Areas of myocardium not taking up the stain were considered to be infarcted. A total of 18 samples were obtained for ^{18}F counting from each animal. In Table 2, the data for infarct:normal myocardium and infarct:blood ratios, as well as the maximum %ID/g uptake in the infarct are summarized. The highest level of ^{18}F accumulation in infarcted tissue was achieved in animals injected with Fab labeled using HPLC-purified [^{18}F]SFBS. Infarct:normal myocardium tissue uptake ratios for these animals were as high as 11.9:1; however, infarct:blood ratios at 2–3.5 hr were only 1.0 to 1.6:1. Maximum target-to-non-target ratios were seen with antimyosin F(ab')$_2$. With this fragment, infarct:normal myocardium ratios as high as 20.6:1 and infarct:blood ratios as high as 3.2:1 were achieved. Myocardial tissue uptake data for all samples obtained from Dog 1, injected with the F(ab')$_2$ fragment, and Dog 3, injected with the Fab fragment, are shown in Figures 1 and 2, respectively. In samples from normal myocardium, uptake in endocardium, midmyocardium and epicardium were quite similar. In general, uptake in samples from the border and infarcted regions was highest in the endocardium and lowest in the epicardium.

TABLE 2
Tissue Distribution Data for ^{18}F-Labeled Antimyosin Mab Fragments

Animal no.*	Slice number	%ID/g Infarct	Infarct: Normal myocardium	Infarct: Blood
F(ab')$_2$ Fragment				
1	A	2.94×10^{-2}	16.0	2.2
	B	3.85×10^{-2}	20.6	2.9
2	A	2.42×10^{-2}	12.1	2.8
	B	2.73×10^{-2}	12.6	3.2
Fab Fragment				
3	A	4.80×10^{-2}	11.9	1.5
	B	5.00×10^{-2}	11.3	1.5
4	A	3.89×10^{-2}	10.9	1.3
	B	3.27×10^{-2}	8.7	1.1
5	A	3.76×10^{-2}	5.3	1.0
	B	6.06×10^{-2}	8.4	1.6

* With the exception of Dog 5, which was killed at 3.5 hr postinjection, these data were obtained at 2 hr.

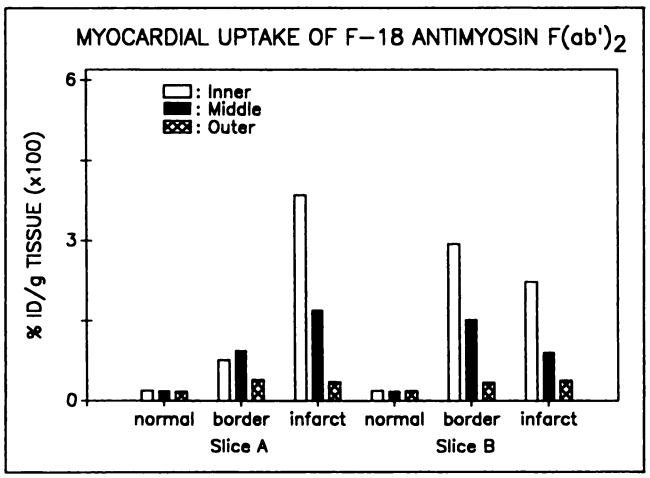

FIGURE 1. Uptake of ^{18}F-labeled antimyosin F(ab')$_2$ in myocardial tissue samples obtained from Dog 1 at 2 hr.

In the PET scans performed on Dogs 2–5, there was a suggestion of increased accumulation of ^{18}F activity in regions of the myocardium expected to be at risk in this model. Delineation of areas of infarcted tissue was complicated by the presence of high levels of ^{18}F activity in the blood pool. In the last dog studied, ^{13}N-ammonia perfusion images were acquired prior to injection of ^{18}F-labeled antimyosin Fab in order to define more clearly the regions with compromised perfusion resulting from left circumflex coronary artery occlusion. By means of the ^{13}N-ammonia perfusion and reperfusion images, ROIs were set. Regions 9, 10, and 11 were in the left anterior descending coronary artery distribution, had relatively high uptake, and were considered to represent normal myocardium; regions 3, 4,

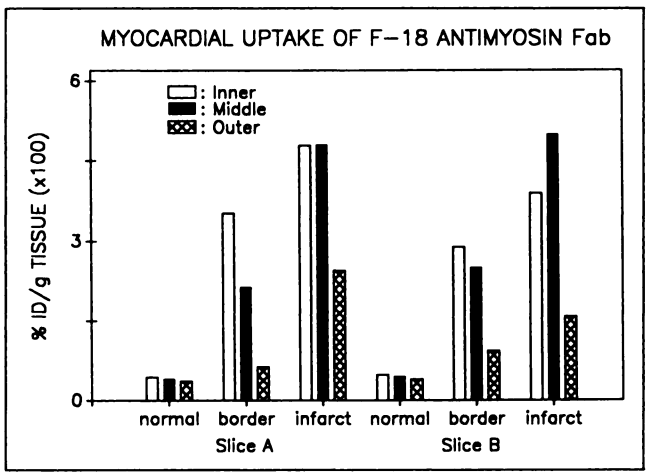

FIGURE 2. Uptake of ^{18}F-labeled antimyosin Fab in myocardial tissue samples obtained from Dog 3 at 2 hr.

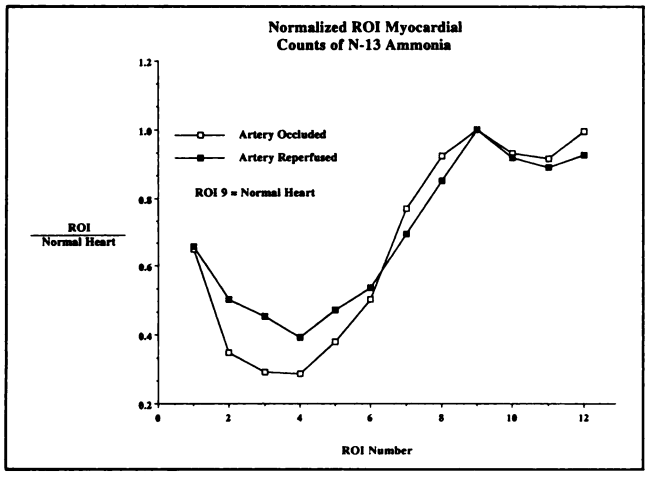

FIGURE 3. Normalized ROI counts of ^{13}N-ammonia in myocardium during occlusion and after reperfusion. Regions 9, 10, and 11 were considered to represent normal myocardium and regions 3, 4, and 5 had lowest activity and were considered to contain infarcted tissue.

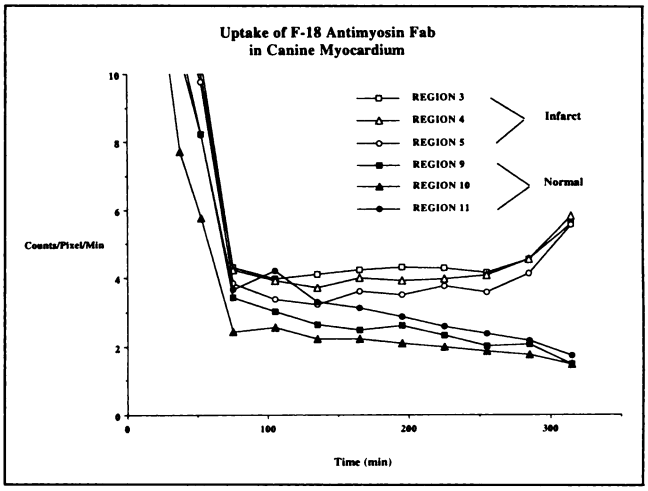

FIGURE 5. Uptake of ^{18}F-labeled antimyosin Fab in regions of normal and infarcted canine myocardium determined from serial PET images from Dog 6.

and 5 had the lowest activity levels and were considered to contain infarcted tissue (Fig. 3). The perfusion to regions 3, 4, and 5 was observed to increase approximately two-fold compared to the occluded flow.

The ^{13}N-ammonia and 315-min Fab images with and without demarcation of these six ROIs are compared in Figure 4. Without the ^{13}N-ammonia image, separation of infarct and blood-pool activity would have been difficult. In Figure 5, the uptake of ^{18}F activity after injection of ^{18}F-labeled Fab in regions of infarcted and normal myocardium (as defined by ^{13}N-ammonia) is plotted as a function of time. Infarct:normal myocardium uptake ratios calculated from these images increased from 1.5:1 at 1 hr to 4.0:1 at 4 hr.

DISCUSSION

The use of receptor-avid tracers for the identification and quantitation of physiologic changes in receptors has been an active area of research in PET. A conceptually similar approach for selective identification of specific cell populations is radiolabeled Mab imaging. Applications of Mab imaging are most common in cancer detection; however, antimyosin Fab and F(ab')$_2$ fragments have been labeled with ^{111}In, ^{99m}Tc, and ^{123}I and used to localize experimental and clinical myocardial infarcts (*11–13,18*). With ^{111}In-labeled antimyosin Fab, myocardial necrosis was detected in 96% of patients with acute myocardial infarction (*13*). Use of single-photon tomographic imaging techniques with ^{99m}Tc-labeled Fab was shown to help increase the detectability of small inferior infarcts (*18*).

Encouraged by these results, we were interested in combining the specificity of Mabs directed against cardiac myosin with the imaging and quantitative advantages inherent in PET. This preliminary investigation was undertaken to determine whether sufficient contrast between uptake in infarcted tissue and both normal myocardium and blood pool could be achieved in a time frame compatible with the 1.8-hr half-life of ^{18}F. Because Mab fragments clear more rapidly from the blood pool than intact

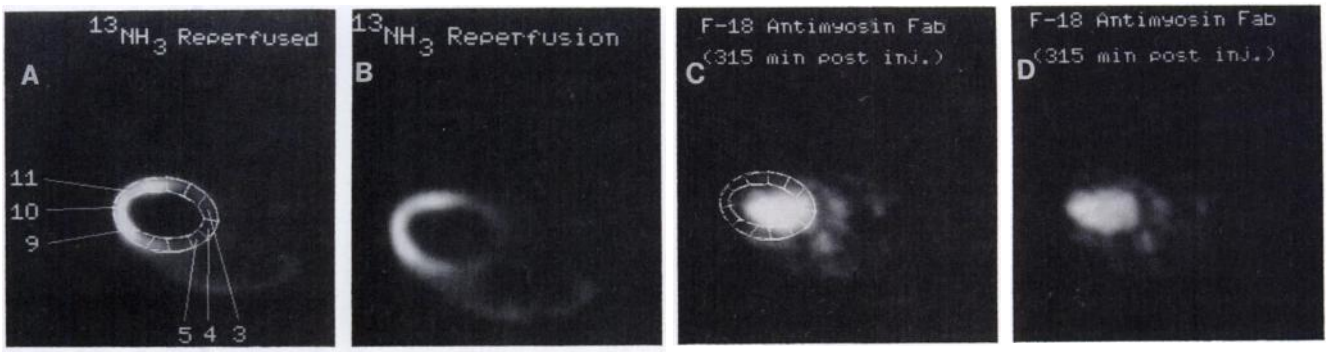

FIGURE 4. Transaxial PET images of Dog 6 with (A and C) and without (B and D) delineation of three normal and three infarcted regions as determined in Figure 4. Both the ^{13}N-ammonia reperfusion (A and B) and ^{18}F-labeled antimyosin Fab images obtained 315 min after administration are shown.

Mabs, Fab and F(ab')$_2$ fragments were used. Even with radiolabeled antimyosin Mab fragments, the optimal time for imaging is generally about 24 hr; however, scintigraphic detection of myocardial infarction as early as 5 hr after injection of labeled Fab has been reported (*11,13,18,19*).

Antimyosin Mab fragments were labeled by reaction with [^{18}F]SFBS. Antimyosin F(ab')$_2$ labeled using HPLC-purified acylation agent was not used in this preliminary study because its clearance from the blood would be too slow to be useful with ^{18}F. Although optimal immunoreactivity and protein coupling efficiency require HPLC purification of the ^{18}F-labeled acylation agent, use of unpurified [^{18}F]SFBS has been shown to reduce blood-pool activity in normal mice (*17*). For example, not using HPLC to purify [^{18}F]SFBS decreased blood-pool activity at 2 hr by a factor of 1.6 for antimyosin Fab and by 4.5-fold for F(ab')$_2$. The more pronounced difference with F(ab')$_2$ is probably due to a greater degree of protein cross-linking with that fragment. Myocardial infarct-to-blood ratios at death were highest in animals receiving ^{18}F-labeled antimyosin F(ab')$_2$. In mice, the decreases in blood-pool activity could be related to corresponding increases in liver uptake (*17*). It would be preferable to avoid excess tracer accumulation in the liver for myocardial imaging, particularly for small inferior infarcts. However, activity in the blood pool would be expected to be a greater problem than liver background with PET imaging.

The most encouraging aspect of the current study is the demonstration that preferential uptake of ^{18}F-labeled antimyosin fragments in infarcted myocardium could be achieved as early as 2 hr after injection. Comparison with results obtained previously for Mab fragments labeled with other nuclides is complicated by the fact that the earliest time points reported generally are at 24 hr. With radiolabeled Fab, infarct:normal myocardium ratios at 24 hr of 14:1 for ^{99m}Tc (*11*), 4 to 11:1 for ^{123}I (*19*) and 2.7:1 for ^{66}Ga (*20*) have been observed in canine reperfused infarct models. With ^{123}I-labeled intact antimyosin Mabs, infarct:normal myocardium ratios of 4:1 for Mab 1B2 and 7 to 20:1 for Mab 5C2 were seen at 24 hr (*19*). Despite the fact that the myocardial distribution of the ^{18}F-labeled antimyosin fragments was determined at only 2–3.5 hr, infarct:normal myocardium ratios compared favorably to those reported previously using other radionuclides at later time points. These results indicate that specific uptake of ^{18}F-labeled antimyosin fragments in infarcted myocardium can be achieved within a reasonable time for use with ^{18}F.

With ^{99m}Tc-labeled Fab, an average uptake of 4.3×10^{-2} % ID/g infarct at 24 hr has been reported (*11*). The results which we obtained with ^{18}F-labeled antimyosin Fab at 2–3.5 hr were quite similar. In general, maximal accumulation of ^{18}F activity was observed in the samples from the endocardial layer. Enhanced uptake in endocardial regions of infarct has also been observed by Khaw et al. (*21*) and by Hoberg et al. (*19*). This distribution pattern would be expected, since maximal myocardial damage in this area should occur with this model.

Antimyosin F(ab')$_2$ Fab fragments were used in this study because of their rapid blood clearance. Even omitting HPLC purification of the ^{18}F-labeled protein acylation agent—a strategy that expedites blood clearance, albeit at the expense of immunoreactivity (*17*)—did not result in favorable infarct:blood ratios. A recent abstract (*22*) has reported that by using sFv fragments of antimyosin, higher infarct:blood ratios could be obtained at early time points without compromising the magnitude of infarct accumulation. These preliminary results suggest that this 26,354 Dalton fragment might be more suited for use with ^{18}F than either Fab or F(ab')$_2$ fragments, and evaluation of ^{18}F-labeled antimyosin sFv is being planned.

In summary, specific uptake of ^{18}F-labeled antimyosin Mab fragments in infarcted myocardium was achieved in a time frame compatible with the half-life of this nuclide. However, prolonged retention of ^{18}F activity in the blood pool interfered with PET imaging. Performance of ^{13}N-ammonia imaging prior to Mab fragment administration to determine regions of poor perfusion allowed infarct:normal myocardium uptake ratios to be calculated from the Mab images which increased with time, reaching a value of 4:1 by 4 hr. Another strategy to be investigated for enhancing hot-spot imaging of damaged myocardium using ^{18}F-labeled antimyosin Mab fragments will be to perform blood-pool subtraction with [^{15}O]carbon monoxide. The results of this preliminary study suggest that imaging of damaged myocardium using PET and ^{18}F-labeled antimyosin fragments may be possible, but some form of blood-pool subtraction or use of sFv fragments will probably be required.

ACKNOWLEDGMENTS

The authors wish to thank Sharon Hamblen, Thomas Hawk, and David Coates for help with the imaging studies. The secretarial assistance of Sandra Gatling and the editorial work of Ann Tamariz are greatly appreciated. We also thank Dr. David Shealy of Centocor for providing the antimyosin antibody fragments. This work was supported in part by Department of Energy grant DE-FG05-89ER60789 and NIH grant P50 HL 17670.

REFERENCES

1. Chilton HM, Hawkins RA, Maddahi J, Phelps ME, Hubner KF, Frick MP. Planning and financing a PET center. *J Nucl Med (SNM Newsline)* 1991;32(4):35N–51N.
2. Bergmann SR, Fox KAA, Rand AL, et al. Quantification of regional myocardial blood flow *in vivo* with $H_2{}^{15}O$. *Circulation* 1984;70:724–733.
3. Shah A, Schelbert HR, Schwaiger M, et al. Measurement of regional myocardial blood flow with N-13-ammonia and positron emission tomography in intact dogs. *J Am Coll Cardiol* 1985;5:92–100.
4. Herrero P, Markham J, Shelton ME, et al. Noninvasive quantification of regional myocardial perfusion with rubidium-82 and positron emission tomography. Exploration of a mathematical model. *Circulation* 1990;82:1377–1386.
5. Sobel BE, Weiss E, Welch M, Siegel B, Ter-Pogossian M. Detection of

remote myocardial infarction in patients with positron emission transaxial tomography and intravenous C-11-palmitate. *Circulation* 1977;55:853–857.
6. Ratib O, Phelps ME, Huang SC, Henze E, Selin CE, Schelbert HR. Positron tomography with deoxyglucose for estimating local myocardial glucose metabolism. *J Nucl Med* 1982;23:577–586.
7. Pike VW, Eakins MN, Allan RM, Selwyn AP. Preparation of [1-^{11}C] acetate—an agent for the study of myocardial metabolism by positron emission tomography. *Int J Appl Radiat Isot* 1982;33:505–512.
8. Martin GV, Caldwell JH, Grunbaum Z, Cerqueira M, Krohn KA. Enhanced binding of the hypoxic cell marker [^{18}F]misonidazole in ischemic myocardium. *J Nucl Med* 1989;30:194–201.
9. Shelton ME, Dence CS, Hwang D-R, Welch MJ, Bergmann SR. Myocardial kinetics of fluorine-18-misonidazole: a marker of hypoxic myocardium. *J Nucl Med* 1989;30:351–358.
10. Khaw BA, Gold HK, Leinbach RC, et al. Early imaging of experimental myocardial infarction by intracoronary administration of I-131-labeled anticardiac myosin F(ab')$_2$ fragments. *Circulation* 1978;58:1137–1142.
11. Khaw BA, Mattis JA, Melincoff G, et al. Monoclonal antibody to cardiac myosin; scintigraphic imaging of experimental myocardial infarction. *Hybridoma* 1984;3:11–23.
12. Khaw BA, Fallon JT, Strauss HW, et al. Myocardial infarct imaging of antibodies to canine cardiac myosin with indium-111-diethylenetriamine pentaacetic acid. *Science* 1980;209:295–297.
13. Khaw BH, Yasuda T, Gold HK, et al. Acute myocardial infarct imaging with indium-111-labeled monoclonal antimyosin Fab. *J Nucl Med* 1987;28:1671–1678.
14. Volpini M, Giubbini F, Gei P, et al. Diagnosis of acute myocardial infarction by indium-111 antimyosin antibodies and correlation with the traditional techniques for the evaluation of extent and localization. *Am J Cardiol* 1989;63:7–13.
15. Nishimura T, Sada M, Sasaki H, et al. Identification of cardiac rejection in heterotopic heart transplantation using ^{111}In-antimyosin. *Eur J Nucl Med* 1987;13:343–347.
16. Yasuda T, Palacios IF, Dec GW, et al. Indium-111 monoclonal antimyosin antibody imaging in the diagnosis of acute myocarditis. *Circulation* 1987;76:306–311.
17. Garg PK, Garg S, Zalutsky MR. Fluorine-18 labeling of monoclonal antibodies and fragments with preservation of immunoreactivity. *Bioconjugate Chem* 1991;2:44–49.
18. Khaw BA, Gold HK, Yasuda T, et al. Scintigraphic quantification of myocardial necrosis in patients after intravenous injection of myosin-specific antibody. *Circulation* 1986;74:501–508.
19. Hoberg E, Eisenhut M, Hofmann M, et al. Monoclonal antibodies specific for human cardiac myosin: selection, characterization and experimental myocardial infarct imaging. *Eur Heart J* 1988;9:328–336.
20. Goethals P, Coene M, Slegers G, et al. Production of carrier-free ^{66}Ga and labeling of antimyosin antibody for positron imaging of acute myocardial infarction. *Eur J Nucl Med* 1990;16:237–240.
21. Khaw BA, Beller GA, Haber E, Smith T. Localization of cardiac antimyosin antibody in myocardial infarction. *J Clin Invest* 1976;58:439–446.
22. Nedelman MA, Shealy D, Boutin R, et al. Rapid infarct imaging with a new Tc-99m antimyosin sFv fragment: evaluation in acute myocardial infarction in dogs [Abstract]. *J Nucl Med* 1991;32:1005.

(continued from p. 569)

SELF-STUDY TEST
Pulmonary Nuclear Medicine
ANSWERS

ITEM 1: Entire Lung Ventilation-Perfusion Mismatch

ANSWER: C

The perfusion images in Figure 1 show almost complete absence of perfusion to the left lung and normal perfusion of the right lung. The ^{81m}Kr ventilation images show only mild impairment of ventilation of the left lung.

Fibrosing mediastinitis, whether idiopathic or secondary to granulomatous infections (typically tuberculosis or histoplasmosis), can lead to central vascular obstruction. In turn, this can produce unilaterally reduced or absent pulmonary perfusion, although obstruction of the superior vena cava is a much more common complication. The bronchi are more resistant to extrinsic compression than are the pulmonary vessels because of their rigid cartilaginous rings. Hence, perfusion is more severely impaired than ventilation in most cases where there is mediastinal fibrosis or mass.

Pulmonary embolism is not likely in this case. Because emboli are usually multiple and bilateral, it would be unusual to observe a massive embolus entirely occluding flow to one lung without detecting any perfusion deficit in the other lung.

Both bronchial adenoma and Swyer-James syndrome would be expected to cause more severe impairment of ventilation than of perfusion in the affected lung. The same would also be true of the regional (segmental) abnormalities seen with asthma; further, unilateral involvement with asthma would be highly unlikely.

Reference

1. Kim EE, DeLand FH. V̇/Q̇ mismatch without pulmonary emboli in children with histoplasmosis. *Clin Nucl Med* 1978;3:328–330.

ITEM 2: Pulmonary Embolism with Bronchoconstriction

ANSWER: E

The repeat study 10 days later (Fig. 2) shows almost complete resolution of the ventilatory abnormalities with significant, but lesser, improvement in the perfusion defects. Thus, pulmonary embolism (with early, acute bronchoconstriction at the time of initial study) is the most likely diagnosis. Bronchospasm due to asthma could have explained the initial findings, but not the persisting perfusion defects at 10 days, when ventilation had returned to normal. Ventilatory abnormality due to emphysema would not have resolved to the extent seen in this patient. There is no evidence to suggest pneumonia, and the scintigraphic abnormalities make anxiety reaction an untenable explanation.

The patient did, in fact, undergo angiography after the first study, and multiple emboli were found. Acute bronchoconstriction due to pulmonary embolism and of sufficient magnitude to cause distinct abnormalities on ventilation imaging is uncommon, but should be considered when multiple segmental perfusion defects are seen and not readily explained by known airways disease.

Reference

1. Kessler RM, McNeil BJ. Impaired ventilation in a patient with angiographically demonstrated pulmonary emboli. *Radiology* 1975; 114:111–112.

ITEM 3 Sarcoidosis

ANSWER: D

The gallium image shown in Figure 3 demonstrates increased uptake of tracer in the lungs and parotid regions. There is also a symmetrical pattern of nodal disease involving the cervical, supraclavicular, hilar, paraaortic, inguinal, and femoral nodes. Bronchogenic carcinoma with lymph node involvement may show pulmonary and mediastinal uptake of ^{67}Ga, as well as gallium localization in distant metastases. However, the symmetry of involvement would be highly unlikely for metastatic disease. Lymphoma is a good possibility, given this patient's history, except that patients with Hodgkin's disease often present with intermittent fever or night sweats. Although gallium uptake in nodal chains and in the lungs is consistent with lymphoma, the high degree of symmetry and the parotid involvement make this diagnostic possibility less likely than sarcoidosis, which is the best fit to the clinical and scintigraphic findings. The pattern of gallium uptake with hypersensitivity pneumonitis or with *Pneumocystis carinii* pneumonia in patients with AIDS rarely includes tracer uptake in the lymph nodes. Generally, there is diffuse pulmonary uptake of moderate to high intensity with *P. carinii* pneumonia and of low to moderate intensity in hypersensitivity pneumonitis. In patients with AIDS, hilar and mediastinal nodal ^{67}Ga uptake may be seen with

(continued on p. 612)